Available online at www.sciencedirect.com
SCIENCE DIRECT®
Physica C 405 (2004) 265–270
PHYSICA C
www.elsevier.com/locate/physc

Magneto-optical study of a single crystal of magnetic superconductor $Sm_{1.85}Ce_{0.15}CuO_{4-x}$

Ruslan Prozorov [a,*], Alexey Snezhko [a], Patrick Fournier [b]

[a] Department of Physics and Astronomy and Nanocenter, University of South Carolina, 712 Main Street, Columbia, SC 29208, USA

[b] Departement de Physique, Canadian Institute of Advanced Research, Centre de Recherche sur les Propriétés Electroniques de Matériaux Avancés, Universite de Sherbrooke, Sherbrooke, Quebec, Canada J1K2R1

Received 22 December 2003; received in revised form 18 February 2004; accepted 20 February 2004
Available online 14 March 2004

Abstract

Low-temperature magneto-optical imaging of a single crystal of magnetic superconductor $Sm_{1.85}Ce_{0.15}CuO_{4-x}$ (SCCO) revealed unusual distribution of the magnetic induction upon magnetic flux penetration and expulsion, implying very low flux pinning. Although some observed features could be compatible with surface or geometric barrier on flux entry, flux exit exhibits distinctively different behavior showing magnetic flux trapped around the sample edge. The role of magnetism in the reduction of pinning is discussed.

PACS: 74.25.−q; 74.72.−h
Keywords: Electron-doped superconductors; Magnetic superconductors; Edge barrier; Magneto-optics

Magneto-optical technique is a powerful method to study distributions of the magnetic induction on the surface of superconductors. Appeared in late 50s [1] and greatly improved in late 60s [2,3], it has become a unique tool for the experimental studies of these materials. The idea behind the technique is to place a transparent magnetic material (an indicator) on the surface of a studied object. Linearly polarized light propagating throughout the indicator and reflected back is rotated proportionally to the magnetization strength along the direction of light (Faraday effect). If indicator is a soft magnetic material, the distribution of the magnetization inside the indicator will mimic the distribution of the perpendicular component of the magnetic induction on the surface of a studied sample. Various indicators were used. For an extensive review of the magneto-optical technique and its applications, see Ref. [4]. The widespread use of magneto-optics for studying high-T_c superconductors started with the advent of so-called in-plane indicators [5–7], which have spontaneous magnetization lying in the indicator plane. Without external magnetic field, there is no Faraday rotation. When perpendicular magnetic

* Corresponding author. Tel.: +1-803-777-8197; fax: +1-803-777-3065.
E-mail address: prozorov@sc.edu (R. Prozorov).

0921-4534/$ - see front matter © 2004 Elsevier B.V. All rights reserved.
doi:10.1016/j.physc.2004.02.011

field is applied, non-zero perpendicular component of the magnetization is induced and the intensity of light through an analyzer (perpendicular to a polarizer) increases proportionally to the applied field strength. When such indicator is placed on a superconductor, distribution of the magnetization inside the indicator is proportional to the distribution of the perpendicular component of the magnetic induction on a superconductor's surface. Therefore, it can be visualized as a real-time two-dimensional optical picture.

This version of the magneto-optical technique has been applied to study Meissner state in high-T_c crystals $YBa_2Cu_3O_7$ (YBCO) where magnetic flux expulsion was observed upon cooling [6,7]. A dome-like shape formation observed in some YBCO crystals (and even untwined parts of the same crystal) was interpreted as interplay of the increasing strength of Meissner currents and pinning forces. In this work, the dome-like shape is also found on flux penetration. Flux exit, however, exhibits different type of irreversible behavior, perhaps due to a novel type of a geometric barrier. Our observations are different from well-known "edge barriers". A common term "edge barrier" is used to designate various mechanisms leading to a delay of vortex penetration, which includes Bean–Livingston barrier due to vortex images as well as geometric barrier appearing in platelet samples of non-ellipsoidal geometry [8–10]. In all cases, the barrier is related to the sample edge—in contrast to the explored here neutral line barrier. The phenomena of the edge barrier has been extensively studied both experimentally and theoretically, see for summary Refs. [8–12]. The signature of the edge barrier is the dome-like shape of the magnetic induction distribution for flux penetration. Experimental methods, which resolved this characteristic dome-like shape in the distribution of a magnetic induction are miniature Hall probes [13–15], bubble-film indicator magneto-optics [16], spattered-film magneto-optics [17], and described above in-plane indicators magneto-optics [18–21]. Bulk pinning competes with the formation of the dome-like shape (not with the barrier itself), thus hampering the observations. Therefore, in most of studies, ultra-clean single crystals were used. Nevertheless, some superconductors, such as borocarbides, exhibit very low bulk pinning [22], probably due to specifics of the layered structure. Edge barrier in borocarbides was studied using miniature Hall-probes in Refs. [13,14]. An increased interest to borocarbides is stimulated, because some of these materials exhibit coexistence of superconductivity with incommensurate antiferromagnetic order [14]. It was suggested that incommensurate antiferromagnetic transition causes an increase in bulk pinning by formed magnetic domains.

In this work we study another magnetic superconductor—$Sm_{1.85}Ce_{0.15}CuO_{4-x}$ (SCCO) which has $T_c \sim 16$ K and a complex magnetic transition at $T_N \sim 4.7$ K [23–25]. There is a ferromagnetic order in the Sm^{3+} layers whereas neighboring layers order antiferromagnetically. The resulting compensation of the exchange field in the location of the superconducting Cu–O planes allows superconductivity to survive. Such arrangement leads to many interesting effects in resistivity, magnetic and thermal responses [24–26], Raman [27], infra-red spectroscopy [27,28] and magnetic penetration depth [29]. Additional interest in this material is stimulated by the ongoing controversy of the pairing type in electron-doped superconductors [30] to which SCCO belongs. Although magnetism impedes direct measurements of the pairing symmetry in this material, there is an overwhelming majority of data in favor of unconventional pairing in electron-doped superconductors [31,32]. This is important for the model, developed in this work, because d-wave superconductors are much more sensitive to magnetism compared to s-wave superconductors.

Single crystals of $Sm_{1.85}Ce_{0.15}CuO_{4-x}$ were grown using a technique described earlier [24]. A sample of $3\times2.5\times0.03$ mm was used in this work. Magneto-optical measurements were conducted using flow-type ^{4}He optical cryostat placed on an X–Y stage of a polarized-light microscope.

Fig. 1 shown penetration and expulsion of the magnetic field into single crystal SCCO after zero-field cooling to 5 K. Left panel, (A–C), shows flux entry, whereas right panel shows flux expulsion. Lighter areas correspond to larger magnetic induction values. Some non-uniformity in the upper right corner of the crystal in due to vacuum

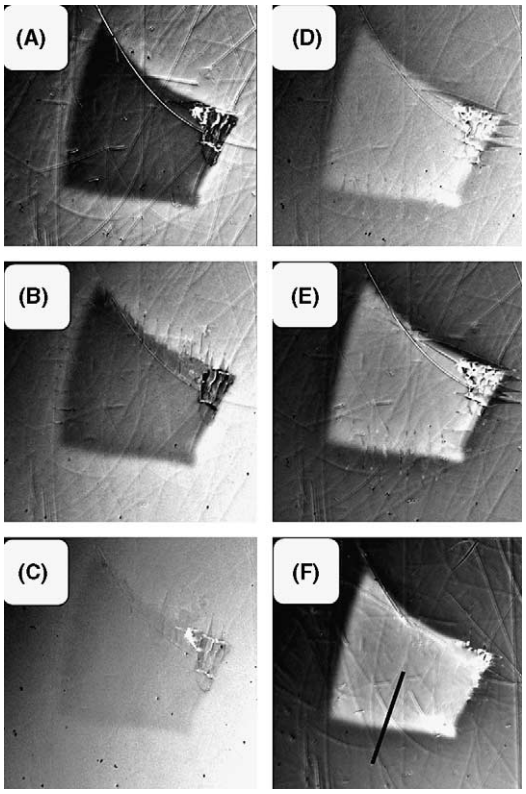

Fig. 1. Magneto-optical images of a single crystal SCCO after zero-field cooling to 5 K. Left panel (A–C) shows increasing magnetic field: (A) 100 Oe, (B) 230 Oe, (C) 700 Oe. Right panel (D–F) shows decreasing field: (D) 230 Oe, (E) 100 Oe, (F) remanent ($H = 0$). The black line in figure (F) corresponds to the area where induction profiles were measured.

grease accidentally got stuck between the sample and the indicator. Some streaks across the images are artifacts of the indicator. The important observation from Fig. 1 is that induction distributions upon flux penetration and flux exit are almost uniform, in a striking contrast with the usual case of bulk pinning where Bean penetration is expected and observed [4]. The observed flux penetration would be consistent with the conventional surface or geometric barrier. However, flux exit is not. This is demonstrated in Fig. 2, which shows magnetic induction profiles for flux penetration after zero-field cooling (left panel) and flux exit (right panel).

The profiles are taken along the line shown in Fig. 1(F). Evidently, the bulk pinning is almost absent and the distribution of the magnetic induction is governed by the edge barrier on flux penetration. However, there is trapped magnetic flux in the remanent state, the dome like shape is not formed and overall distribution of the magnetic induction contradicts simple surface or geometric barrier physics. To underline the difference between flux penetration and flux exit, magnetic induction profiles are plotted on the same graph (Fig. 3) for flux penetration and exit in the external field of 100 Oe.

Magnetic induction peaks are situated well inside the sample (at $\sim$0.3 mm with the sample center at 1.3 mm from the edge). This distance from the edge is too large to be a λ-layer, within which the typical edge barrier would be effective. Most importantly, this barrier works for flux entry as well as for flux exit. Indeed, it could be explained by the enhanced vortex pinning at the perimeter of the sample, but this usually comes from chemical inhomogeneities or surface roughness. Both are noticeable only at much smaller distances from the edge. Moreover, X-ray structural analysis, heat capacity and resistivity measurements did not reveal any inhomogeneities or a second phase. To further emphasize the difference between flux entry and exit, three-dimensional distributions are shown in Fig. 4. The height is proportional to the magnetic induction. Roughly half of the sample is shown—to emphasize the flux structure in the interior. Top picture in Fig. 4 shows three-dimensional distribution on flux penetration, whereas bottom picture shows trapped flux. Evidently, the distribution of flux is quite uniform and, therefore, cannot be attributed to some spurious effects.

We propose an alternative explanation of the observed effect. In SCCO, magnetic field intensity in the vortex core is sufficient to polarize Sm^{3+} spins. These magnetic moments contribute to the total flux curried by the vortex and produce self-field, which must be screened by the superconductor. Since total flux of the vortex must be one flux quanta, ϕ_0, shielding currents around the vortex are reduced. As a result, London penetration depth significantly increases [29]. It is also possible that enhanced pair-breaking in the vortex core would lead to the decrease of the coherence length. Both effects lead to the suppression of

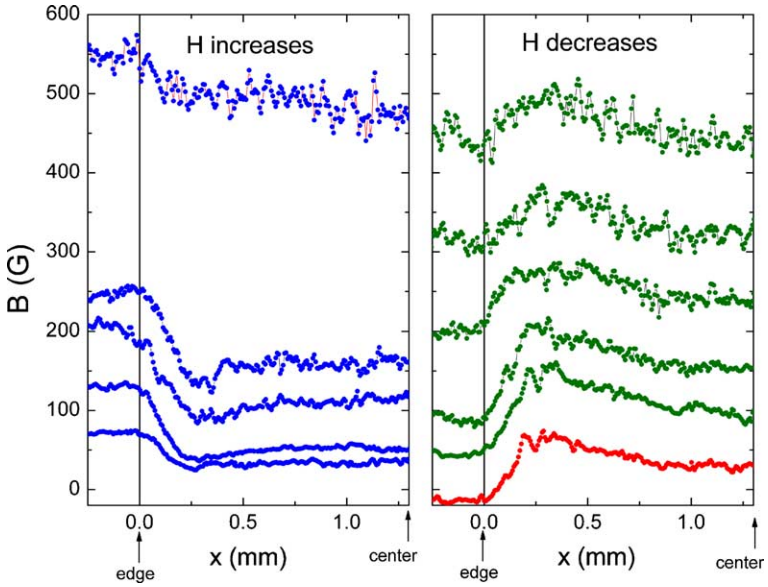

Fig. 2. Magnetic flux penetration (left panel) and magnetic flux exit (right panel).

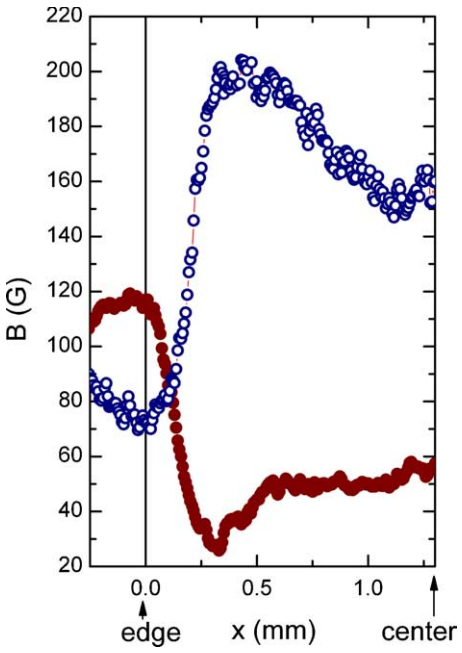

Fig. 3. Profile of magnetic induction for flux penetration (solid symbols) and exit (open symbols) for the external field of 100 Oe.

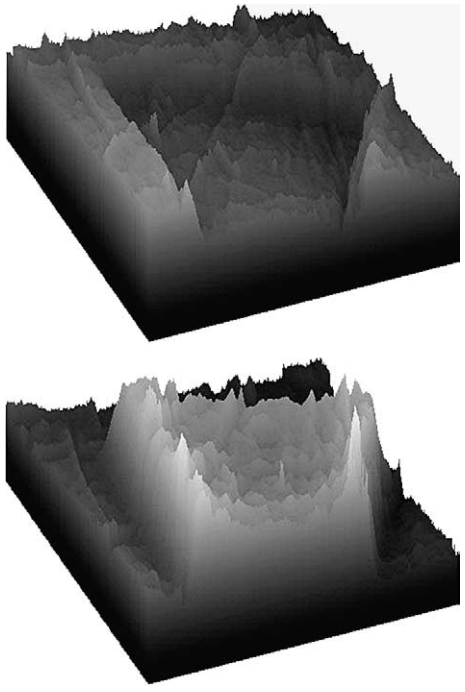

Fig. 4. Three-dimensional distribution of the magnetic induction upon flux penetration (top) and flux exit (bottom) shown for half of the sample (the cross-section plane faces the reader).

vortex pinning. Transverse (in-plane) component of the magnetic field, which leads to vortex bending in platelet samples would also lead to Sm^{3+} spins deviation from the antiferromagnetic cancellation on the Cu–O planes. However, since this field is parallel to the Cu–O plane, it does not cause significant suppression of the superconducting order parameter due to the absence of the orbital effects. This situation makes vortex pinning to become extremely angle dependent.

There are several possible reasons for the concentration of magnetic flux upon flux exit. Similar effect has been previously observed for samples with weak bulk pinning [33]. The trivial explanation is imperfections and enhanced defect structure at the sample edges. However, this mechanism is unlikely due to very uniform shielding in the Meissner state. Edge defects usually result in dendrite-like penetration of the magnetic flux. Another possibility could be related to the platelet geometry of the sample and vortex bending. This effect is somewhat similar to the intrinsic pinning in layered superconductors where vortex bending could explain the zero-field peak in magnetization loops [34,35]. With significant anisotropy of pinning enhanced by the magnetic component, the distribution of vortex density would behave irreversibly when magnetic field is decreased and a region around neutral line will retain trapped vortices upon flux exit. According to our model, at large fields ($H \gg H_{c1}$, when vortex bending is negligible) almost uniform Bean current is achieved. Upon subsequent reduction of external field, vortices around neutral line remain pinned, as seen in Figs. 2 and 3 and ultimately trapped (Fig. 4) thus forming an apparent barrier for flux exit. Indeed, more rigorous calculations are needed and alternative explanations for the observed effect should be considered.

Acknowledgements

We thank R.W. Giannetta for useful discussions. Work at the University of South Carolina was supported by the NSF/EPSCoR under grant no. EPS-0296165. Work at the Université de Sherbrooke was supported by CIAR, CFI, the Natural Sciences and Engineering Research Council of Canada, and the Foundation of the Université de Sherbrooke.

References

[1] P.B. Alers, Phys. Rev. 105 (1957) 104.
[2] H. Kirchner, Phys. Lett. A 30 (1969) 437.
[3] R.P. Huebener, V.A. Rowe, R.T. Kampwirth, J. Appl. Phys. 41 (1970) 2963.
[4] C. Jooss, J. Albrecht, H. Kuhn, S. Leonhardt, H. Kronmueller, Reports on Progress in Physics 65 (2002) 651.
[5] L.A. Dorosinskii, M. Indenbom, V.I. Nikitenko, Y.A. Ossip'yan, A.A. Polyanskii, V.K. Vlasko-Vlasov, in: A.A. Aronov, A.I. Larkin, V.S. Lutovinov (Eds.), High Temperature Superconductivity and Localization Phenomena, World Scientific, Singapore, 1991, p. 503.
[6] V.K. Vlasko-Vlasov, L.A. Dorosinskii, M.V. Indenbom, V.I. Nikitenko, A.A. Polyanskii, R.L. Prozorov, Sverkhprovodimost: Fizika, Khimiya, Tekhnika 5 (1992) 2017.
[7] L.A. Dorosinskii, V.I. Nikitenko, A.A. Polyanskii, R.L. Prozorov, V.K. Vlasko-Vlasov, Physica C: Superconductivity and its Applications, Amsterdam, Netherlands, 206 (1993) 360.
[8] E.H. Brandt, Reports on Progress in Physics 58 (1995) 1465.
[9] E. Zeldov, Phys. Rev. Lett. 73 (1994) 1428.
[10] T. Schuster, Phys. Rev. Lett. 73 (1994) 1424.
[11] A.M. Campbell, J.E. Evetts, Critical Currents in Superconductors, Taylor and Francis Ltd., London, 1972.
[12] E.H. Brandt, Phys. Rev. B 60 (1999) 11939.
[13] S.S. James, C.D. Dewhurst, R.A. Doyle, D.M. Paul, Y. Paltiel, E. Zeldov, A.M. Campbell, Physica C: Superconductivity and its Applications, Amsterdam, 332 (2000) 173.
[14] S.S. James, C.D. Dewhurst, S.B. Field, D.M. Paul, Y. Paltiel, H. Shtrikman, E. Zeldov, A.M. Campbell, Phys. Rev. B 64 (2001) 092512.
[15] D.A. Brawner, N.P. Ong, J. Appl. Phys. 73 (1993) 3890.
[16] Z.W. Lin, G.D. Gu, G.J. Russell, Supercond. Sci. Technol. 13 (2000) 1170.
[17] H. Castro, B. Dutoit, A. Jacquier, M. Baharami, L. Rinderer, Phys. Rev. B 59 (1999) 596.
[18] H. Bocuk, L. Dorosinskii, U. Topal, Physica C: Superconductivity and its Applications, Amsterdam, Netherlands, 377 (2002) 561.
[19] M.W. Gardner, S.A. Govorkov, R. Liang, D.A. Bonn, J.F. Carolan, W.N. Hardy, J. Appl. Phys. 83 (1998) 3714.
[20] M.V. Indenbom, C.J. Van Der Beek, V. Berseth, M. Konczykowski, F. Holtzberg, W. Benoit, Czec. J. Phys. 46 (1996) 1541.
[21] M.V. Indenbom, G. D'Anna, M.O. Andre, V.V. Kabanov, W. Benoit, Physica C 235–240 (1994) 201.
[22] R. Prozorov, E.R. Yacoby, I. Felner, Y. Yeshurun, Physica C: Superconductivity, Amsterdam, 233 (1994) 367.

[23] S.J. Hagen, J.L. Peng, Z.Y. Li, R.L. Greene, Phys. Rev. B 43 (1991) 13606.
[24] J.L. Peng, Z.Y. Li, R.L. Greene, Physica C 177 (1991) 79.
[25] B.K. Cho, J.H. Kim, Y.J. Kim, B.-h. O, J.S. Kim, G.R. Stewart, Phys. Rev. B 63 (2001) 214504/214501.
[26] R.F. Jardim, C.H. Westphal, C.H. Cohenca, L. Ben-Dor, M.B. Maple, J. Appl. Phys. 79 (1996) 6564.
[27] E.-M. Choi, M.-O. Mun, I.-S. Yang, Y.J. Kim, J.H. Kim, S.R. Park, W.T. Kim, S.H. Rha, B.-h. O, J. Korean Phys. Soc. 34 (1999) 292.
[28] R. Kannan, S. Mohan, Talanta 53 (2001) 733.
[29] R.W. Giannetta, R. Prozorov, P. Fournier, D.D. Lawrie, in preparation.
[30] P. Fournier, E. Maiser, R.L. Greene, NATO ASI Series, Series B: Physics 371 (1998) 145.
[31] R. Prozorov, R.W. Giannetta, P. Fournier, R.L. Greene, Phys. Rev. Lett. 85 (2000) 3700.
[32] C.C. Tsuei, J.R. Kirtley, Phys. Rev. Lett. 85 (2000) 182.
[33] B. Khaykovich, Physica C 235–340 (1994) 2757.
[34] L.W. Conner, A.P. Malozemoff, Phys. Rev. B 43 (1991) 402.
[35] L.W. Conner, A.P. Malozemoff, I.A. Campbell, Phys. Rev. B 44 (1991) 403.